Cancer Science
Volume 112, Issue 11 p. 4478-4489
ORIGINAL ARTICLE
Open Access

# MK-6, a novel not-α IL-2, elicits a potent antitumor activity by improving the effector to regulatory T cell balance

Maki Kobayashi, Katsuhiko Kojima, Kazutaka Murayama, Yuji Amano, Takashi Koyama, Naoko Ogama, Toshikazu Takeshita, Tatsuro Fukuhara, Nobuyuki Tanaka
First published: 20 September 2021
https://doi.org/10.1111/cas.15127
About

## Abstract

IL-2 is a pleiotropic cytokine that regulates immune cell homeostasis. Its immunomodulatory function has been used clinically as an active immunotherapy agent for metastatic cancers. However, severe adverse effects, including the vascular leak syndrome and the preferential stimulation of anti-immunogenic Treg rather than effector T cells, have been obstacles. We newly designed a mutein IL-2, Mutakine-6 (MK-6), with reduced IL-2Rα–binding capability. MK-6 induced comparable cell growth potential toward IL-2Rβγ–positive T cells but was far less efficient in in vitro Treg proliferation and STAT5 activation. Unlike IL-2, in vivo administration of MK-6 produced minimal adverse effects. Using CT26 and B16F10-syngeneic tumor models, we found MK-6 was highly efficacious on tumor regression. Serum albumin conjugation to MK-6 prolonged in vivo half-life and accumulated in CT26 tumors, showing enhanced antitumor effect. Tumor-infiltrating leukocytes analysis revealed that albumin-fused MK-6 increased the ratio of effector $CD8^+$ T cells to $CD4^+$ Treg cells. These results demonstrated that MK-6 is an efficient immunomodulator potentially used for improved immunotherapy with decreased adverse effects and attenuated Treg stimulation.

## Abbreviations

- ALT
  - alanine transaminase
- AST
  - aspartate transaminase
- AUC
  - area under the curve
- CT26
  - colon tumor 26
- $EC_{50}$
  - effective concentration 50
- EPR
  - enhanced permeability and retention of macromolecules
- IL-2
  - interleukin-2
- IL-2Rs
  - interleukin-2 receptors
- MSA
  - mouse serum albumin

- TME
  - tumor microenvironment
- TIL
  - tumor-infiltrating lymphocyte
- Treg
  - regulatory T cells
- VLS
  - vascular leak syndrome

# 1 INTRODUCTION

IL-2 is a crucial cytokine maintaining the homeostasis of lymphocytes. The functions of IL-2 are pleiotropic, and it exerts both stimulatory and regulatory roles in the immune system.[1-3] Functional IL-2 receptors (IL-2Rs) are either trimeric receptors composed of IL-2Rα (CD25), IL-2Rβ (CD122), and IL-2Rγ (the common cytokine receptor g chain; γc, CD132) chains or dimeric βγ IL-2Rs.[4, 5] Both of these receptor complexes transmit signals via the JAK3-STAT5 pathway. The trimeric IL-2Rαβγ forms high-affinity receptors with roughly 10-100 times higher affinity for IL-2 than the intermediate-affinity dimeric βγ IL-2Rs.[6] Naïve $CD8^+$ T, antigen-experienced (memory) $CD8^+$ T, and natural killer (NK) cells express dimeric βγ IL-2Rs. IL-2Rα by itself serves as a low-affinity nonsignaling receptor, sequestering IL-2 in the tissue or contributing as an affinity converter for the intermediate IL-2Rs. Activated lymphocytes inducibly express IL-2Rα to form the trimeric αβγ IL-2Rs. In this regard, regulatory T cells (Tregs) are distinct for their constitutive positivity for high-affinity IL-2Rs.[7-9] Thus, IL-2Rα expression is an active determinant on tissue distribution/sequestration of IL-2 and efficient signal transmission[3] and a fate changer for responder cells.[8, 10]

The FDA approved a recombinant IL-2 (Aldesleukin) in 1992 as the first cancer immunotherapy agent in clinical use. The patients with metastatic melanoma and renal cell carcinoma who received high-dose IL-2 experienced a long-term impact on overall survival.[11, 12] Despite these outcomes, IL-2–based approaches often induce systemic toxicity, the vascular leak syndrome (VLS). Damage of endothelial cells and vasculatures leads to fatal vascular leakage resulting in multiple organ failures. Notably, direct interaction between IL-2 with IL-2Rα on endothelial cells in the lungs leads to severe pulmonary edema.[13] The expansion of Treg by IL-2 seems to limit its therapeutic efficacy. Low dose IL-2 may affect the preferential proliferation of Treg rather than memory $CD8^+$ T and NK cells, leading to an undesirable immune balance shift to antitumor immunity.[2, 14] Therefore, designing a “biobetter” IL-2 has been a challenge.

This study designed a genetically modified not–α-binding human IL-2 Mutein, Mutakine-6 (MK-6). MK-6 preserves $CD8^+$ T cell proliferation potential without robust expansion of Treg. We demonstrate an improved Mutein property that upregulates the effector to Treg cell balance in preclinical models.

# 2 MATERIALS AND METHODS

## 2.1 Cell lines

293T and Expi293F were purchased from ATCC and Thermo Fisher Scientific, respectively. CT26, B16F10, and CTLL-2 were purchased from Riken Bioresource Center. I. Miyoshi provided MT-2, and T. Takeshita gifted TPA-Mat, TPA-Mat αKO, and KHYG-1. See Appendix S1 for detailed culture conditions, plasmids, and transfections.

## 2.2 Mice

Female BALB/c and C57BL/6 mice, 6- to 7-week-old, were purchased from CLEA Inc. All mice were maintained under specific pathogen-free conditions following guidelines for animal experimentation. All

animal studies were performed according to the guidelines of animal ethics and approved by the Miyagi Cancer Center Animal Care and Use Committee (permit number: MCCAE-2020-10 and AE.21.04).

## 2.3 Homology modeling of MK-6, MK-9, and MK-18

We built the homology model of MK-6, MK-9, and MK-18 by using MODELLER[15] with the standard protocol. The IL-2 structure (PDB-ID: 2ERJ, chain-D) was used for the template model to produce the sequence alignment between Thr3-Thr133 for IL-2 and Ala3-Thr133 for MK-6. We used MolFeat (FiatLux) to depict the molecular structures (ribbon and molecular surface models).

## 2.4 In vitro T cell proliferation assay

We added indicated concentrations of Mutakines either to CTLL-2 or TPA-Mat cells. Seventy-two hours later, cell numbers were assessed as ATP content (CellTiter-Glo, Promega).

## 2.5 STAT5 phosphorylation (pSTAT5) and Treg stimulation assays

We stimulated MT-2 ($1 \times 10^6$) with Mutakines and performed Western blots as described previously using anti-STAT5 and anti-phospho-STAT5 (Tyr694; pSTAT5) Abs (CST).[16] For ex vivo proliferation assays, we labeled Tregs with 5(6)-carboxyfluorescein diacetate succinimidyl ester (CFSE) and stimulated them with anti-CD3 and anti-CD28 Abs and increasing concentrations of Mutakines. Seventy-two hours later, CFSE dilution and the mean fluorescence intensity (MFI) of FoxP3 were determined. See Appendix S1 for Treg preparation.

## 2.6 Assessment of treatment-associated toxicity in vivo

Either MK-0 (2.5, 25, and 250 μg) or MK-6 (2.5, 25, 100, and 250 μg) were intraperitoneally administered to BALB/c mice once a day for 4 days. On day 5, we sacrificed the mice to measure body weight, liver weight, and pulmonary wet to dry weight ratio using a miVac (SP Scientific). Oriental Yeast Ltd. determined serum aspartate transaminase (AST) and alanine transaminase (ALT) concentrations.

## 2.7 Syngeneic mouse tumor models

CT26 cells ($5 \times 10^5$/mouse) were injected intradermally into the back of BALB/c. We caliper-measured tumor sizes and estimated the volume by the formula: $V = 0.5 \times (\text{shortest diameter})^2 \times (\text{longest diameter})$. CT26-bearing mice were randomized on day 5 and administered with MK-6, MK-0, MSA-MK6, or MSA-MK0. For B16F10 melanoma models, $5 \times 10^5$ B16F10 cells were injected intradermally into the back of syngeneic C57BL/6 mice. For details, see Appendix S1.

## 2.8 Statistical analyses

Two-group datasets were analyzed by Student's *t*-test (GraphPad Prism5). For three- or more-group analysis, one-way ANOVA followed by Tukey's post hoc test and $P = .05$ was considered to be significantly different ($^{*}P < .05$, $^{**}P < 0.01$, $^{***}P < 0.001$, $^{****}P < 0.0001$).

# 3 RESULTS

## 3.1 Design and screening for not–IL-2Rα–binding Mutakines

To obtain an IL-2 mutant (Mutakine) with attenuated Treg activation and adverse effects, we aimed to decrease IL-2Rα–binding capability. As a starting IL-2 protein template, we selected an aldesleukin-type IL-2 (MK-0) harboring a Thr 3 to Ala (T3A) and a C125A mutation that avoids O-glycosylation–

dependent heterogeneity and aggregation.[4, 17] For the chase analysis, we fused NanoLuc to the C-terminus of IL-2, a portion not participating in any receptor interactions (Figure S1). By appending a signal sequence,[18] we managed to purify the NanoLuc-MK-0 hybrid protein. Based on the crystal structure showing the human IL-2/IL-2R complex (Figure S2),[4, 19] multiple interactions between IL-2 and IL-2Rα, including K35A, F42A, Y45A, and L72G, were our significant targets for mutations (Figure S3). These critical residues on IL-2 are conserved between humans and mice, suggesting their significance in interface formation. We also paid attention not to interfere with the IL-2/IL-2Rβ and IL-2/IL-2Rγ interactions. First, we confirmed that MK-0 possesses a binding capacity for mouse IL-2Rα and CTLL-2 proliferation potential, similar to wild-type IL-2 (MK-0) (Figure S4). We next performed an IL-2Rα–binding assay with candidate Mutakines to examine their reduction in α binding (Figure S5). We added NanoLuc-variant–IL-2 fusion proteins to the 293T expressing IL-2Rα (293Tα) or parental 293T (Figure S6) and evaluated Mutakine's mouse IL-2Rα binding as an index of 293Tα to 293T (Figures 1A,B, S7). Among the 16 Mutakines, four candidates (MK-3, MK-5, MK-6, MK-13) were selected as low binders for IL-2Rα compared with the IL-2Rα binding of MK-0, and highly purified recombinant proteins were prepared (Figure S8A,B). Notably, MK-6 possesses four mutations, K35A/R38A/K43A/Y45A, localized on the IL-2/IL-2Rα interface showing little ability to bind IL-2Rα (mouse 293Tα/293T ratio; MK-0 vs MK-6 = 1425.6 vs 1.8, human 293Tα/293T ratio; MK-0 vs MK-6 = 1733.9 vs 5.2) (Figure 1A,B). Similarly, we confirmed MK-13 with K35A/R38A/L72G mutations has almost lost its IL-2Rα–binding capability.

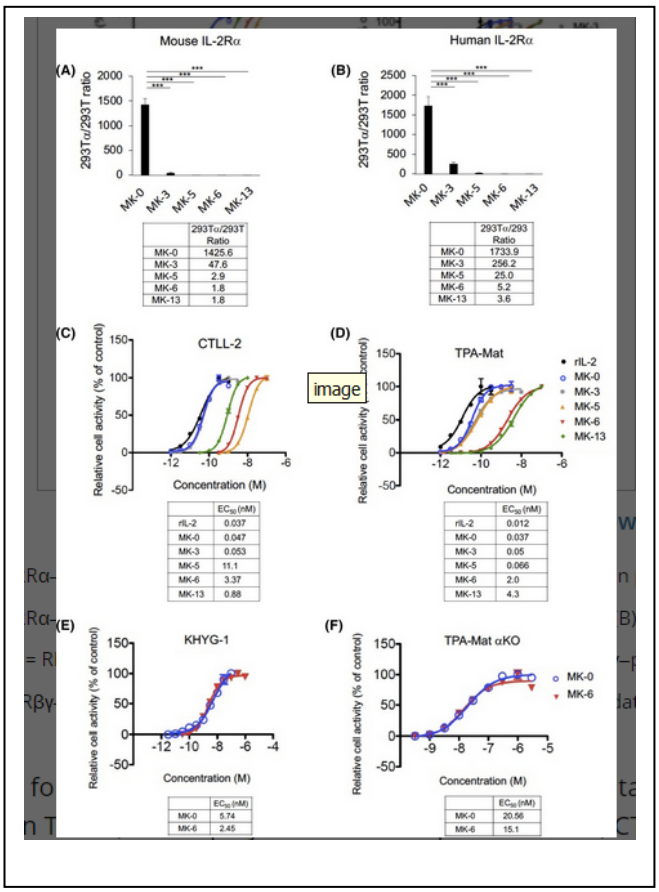


**FIGURE 1**
Open in figure viewerPowerPoint

MK-6 has lost the IL-2Rα–binding capability while maintaining a partial T cell proliferation potential. 293Tα, mouse or human IL-2Rα–introduced 293T. Binding assay on the mouse (A) and human (B) IL-2Rα, calculated as the 293Tα/293T ratio = $RLU^{293T\alpha}/RLU^{293T}$. n = 6 per group. Cell growth assay on IL-2Rαβγ–positive CTLL-2 (C) and TPA-Mat (D), and IL-2Rβγ–positive KHYG-1 (E) and TPA-Mat αKO (F). n = 3 per group. All data show means ± SEM

Next, we checked the four candidates for their function. To confirm Mutakines' growth-promoting capacity on T cells, we employed two IL-2–dependent lines, CTLL-2 and TPA-Mat, expressing mouse and human IL-2Rαβγ, respectively (Figures 1C,D, S9A-D, S10A). MK-3 with a slight residual IL-2Rα–binding capacity rendered good growth potential to both CTLL-2 and TPA-Mat cells, similar to the effects of wild-type IL-2. The half-maximum effective concentration ($EC_{50}$) of MK-5, MK-6, and MK-13 was much higher than IL-2, ranging from 0.88 to 11.1 nmol $L^{-1}$ for CTLL-2 cells. For TPA-Mat, these three Mutakines also gave a higher $EC_{50}$ of 0.066 to 4.3 nmol $L^{-1}$. Based on the minimum IL-2Rα–binding capacity and partial cell proliferation ability on both mouse and human T cells, we finally

selected MK-6. The half-maximum $EC_{50}$ of MK-6 was increased compared with MK-0 on mouse CTLL-2 ($EC_{50}^{MK-0}$ 0.047 nmol $L^{-1}$, $EC_{50}^{MK-6}$ 3.37 nmol $L^{-1}$) (Figure 1C), which was similar to that on human TPA-Mat ($EC_{50}^{MK-0}$ 0.037 nmol $L^{-1}$, $EC_{50}^{MK-6}$ 2.0 nmol $L^{-1}$) (Figure 1D). Next, we performed proliferation assays using two IL-2Rβγ–expressing cell lines, KHYG-1 and TPA-Mat αKO (Figure S10B,C). $EC_{50}^{MK-0}$ and $EC_{50}^{MK-6}$ toward these two cells were similar (Figure 1E,F). Furthermore, to compare MK-6 with other IL-2 muteins, we performed experiments using MK-9, MK-18, and MK-19 carrying the IL-2 mutations from previously reported three muteins, CEA-IL2v,[20] human IL-2 mutein,[21] and superkine,[22] respectively (Figure S11A-G). The results showed that MK-19 has a residual partial affinity toward IL-2Rα, while MK-6, MK-9, and MK-18 have lost the binding capability (Figure S11B,C). The latter three muteins possess comparable growth potential on human IL-2Rβγ–expressing cells (Figure S11D,E). Interestingly, MK-9 and MK-18 could not support murine T cell growth at all (Figure S11G). Taken together, we found MK-6 is one of the best Mutakine in terms of negligible IL-2Rα–binding capacity, but it possesses comparable growth potential toward both human and mouse IL-2Rβγ–expressing cells from the aspect of Emax value.

## 3.2 Structural basis of MK-6 for not–IL-2Rα–binding capability

To verify a structural basis of MK-6 for its inability to bind IL-2Rα, we performed a computer-assisted 3D simulation based on the previously reported crystal structure of the quaternary IL-2-IL-2Rα–IL-2Rβ–γc complex. IL-2 binds to IL-2Rα through hydrogen bonds and Van der Waals contacts between K35, R38, K43, and Y45 localized on the AB loop of the IL-2 surface and IL-2Rα (Figure 2A). The mutations of K35A, R38A, K43A, and Y45A remove large parts of Van der Waals's interaction surface, rendering ineffective binding to IL-2Rα without changing the native IL-2 structure (Figure 2B). Therefore, the overall design of the MK-6–IL-2Rβγ complex remains essentially similar to the wild-type quaternary complex.

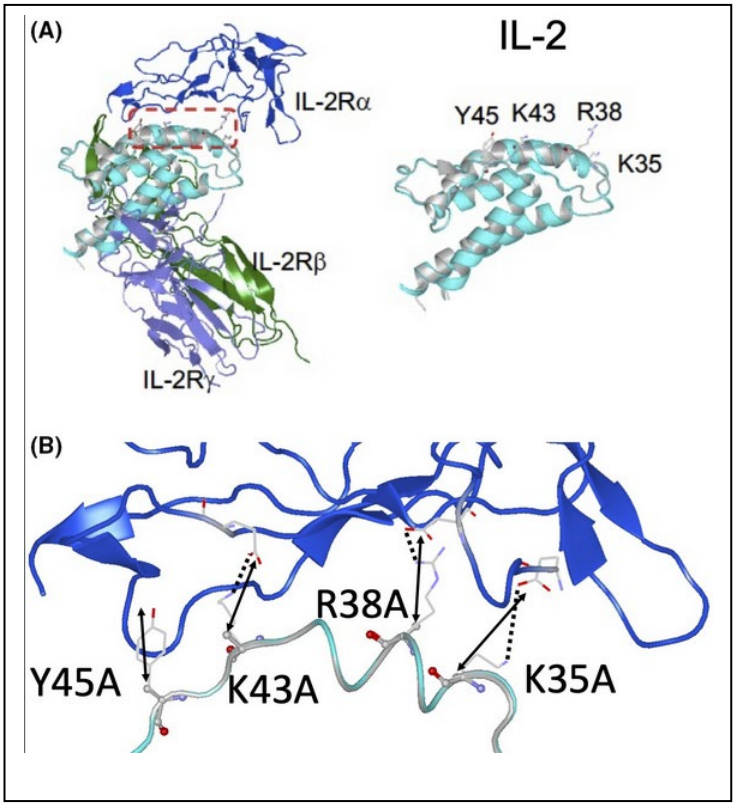


**FIGURE 2**

Open in figure viewerPowerPoint
Model structure of human IL-2 and MK-6 in complex with IL-2Rαβγ. A, Left: ribbon representation of superimposed quaternary complex structure IL-2Rαβγ and MK-6 (IL-2, cyan; MK-6, gray, IL-2Rα, blue; IL-2Rβ, green; IL-2Rγ, purple). Right: mutation sites on MK-6 (close-up on red dashed frame). B, Close-up view onto the loop region between helix-A and helix-B and the binding site MK-6 with human IL-2Rα. The picture shows an overlay of IL-2 (cyan) or MK-6 (gray) IL-2Rα structure. We offer the intermolecular distance of hydrophobic patches with K35A/R38A/K43A/Y45A after transformation to MK-6 (solid arrow). Dashed line shows hydrogen binding to IL-2/IL-2Rα

## 3.3 MK-6 attenuated Treg function in vitro and ex vivo

To examine whether MK-6 has a lower proliferating potential on Treg, we first used human MT-2 cells, showing several Treg characteristic markers, such as FoxP3$^{+}$CD25$^{+}$CD4$^{+}$. With its human IL-2Rαβγ expression and suppressive effects on T cells (Figure S12A-E), we and others regarded MT-2 as a human Treg-like cell line.[23] We stimulated MT-2 with a titrated dose of MK-0 and MK-6 and examined pSTAT5 at a lower amount of MK-0 (0.001 nmol $L^{-1}$). MK-0 increased the phosphorylation levels in a quantity-dependent manner up to 10 nmol $L^{-1}$ (Figure 3A). MK-6, however, induced minor if any pSTAT5 even at a higher concentration of 10 nmol $L^{-1}$. Thus, MK-6 exhibited weaker IL-2–signaling potential on a human Treg-like cell compared with the control.

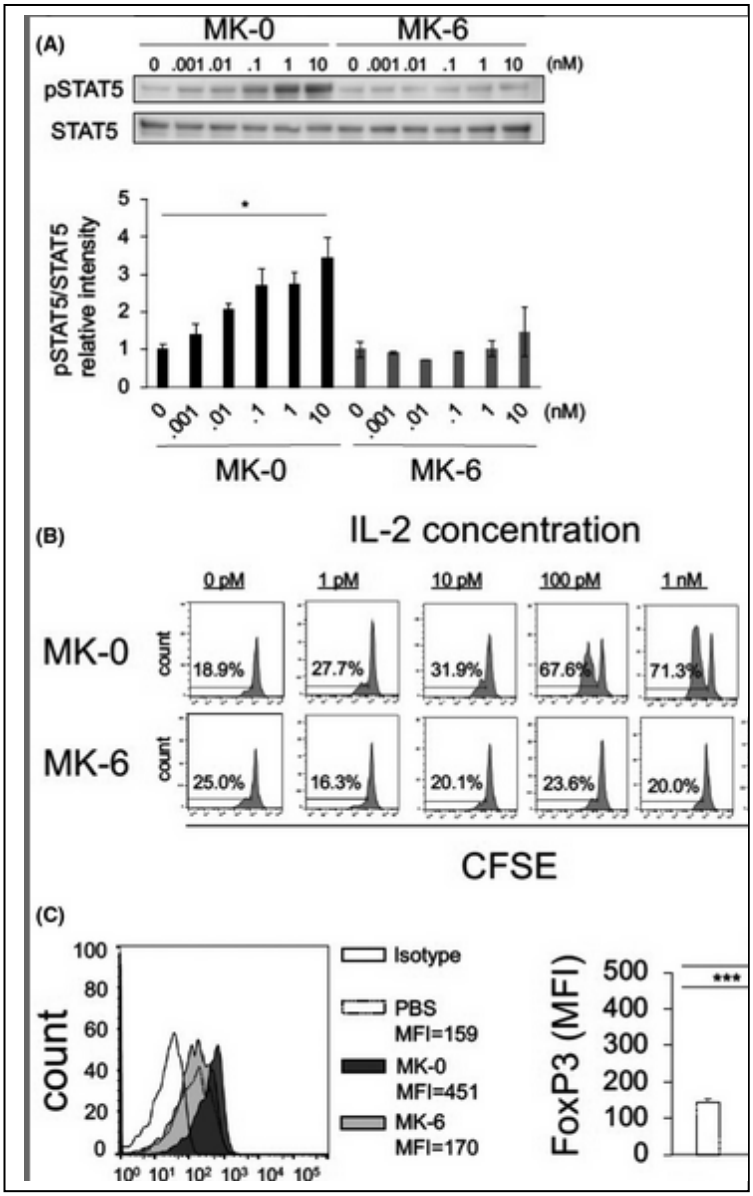


**FIGURE 3**

Open in figure viewerPowerPoint

MK-6 has a weaker ability for proliferation and induction of Treg cells in vitro and ex vivo. A, Upper: Western blot analyses showing the expressions of STAT5 phosphorylation (pSTAT5) in MT-2 after Mutakines' activation. Cells were left unstimulated or stimulated with MK-0 and MK-6 for 15 min and lysed and immunoblotted with anti-pSTAT5 (top) or anti-STAT5 (bottom) Abs. Lower: quantification bar graphs of blot analysis. n = 2 per group. B, Expansion of Treg in vitro. We cultured 5(6)-carboxyfluorescein diacetate succinimidyl ester (CFSE)-labeled, beads-sorted Treg cells with MK-0 and MK-6 at indicated concentrations for 72 h. C, Left: intracellular staining showing the level of FoxP3 expression by beads-sorted Tregs further expanded with MK-0 (dark gray–filled) and MK-6 (bright gray–filled). Isotype (open) and control (dashed line). Right: mean fluorescence intensity (MFI) values for FoxP3. n = 3 per group. Data show means + SEM. NS, not significant

Next, we examined whether MK-6 affects ex vivo Treg proliferation using mouse peripheral CD25$^{+}$CD4$^{+}$ Treg cells isolated from the spleen. We incubated cells with various doses of MK-6 or MK-0 in the presence of anti-CD3/CD28 and monitored cell division by dilution of incorporated CFSE dye. MK-0 initiated Treg cells' proliferation as low as 1 pmol $L^{-1}$, and 10 pmol $L^{-1}$ MK-0 showed a significant CSFE-low fraction appearance (Figure 3B: *upper*). However, 10 pmol $L^{-1}$ of MK-6 induced minor cell division on Treg, and even 1 nmol $L^{-1}$ MK-6 was ineffective. Indeed, we observed Treg cells' proliferation at a very high MK-6 concentration of 10 nmol $L^{-1}$ (Figure 3B: *lower*). Thus, MK-6 presents a significantly weaker ability on Treg proliferation compared with that of MK-0. Next, we examined whether MK-6 possesses attenuated induction of FoxP3, a transcription factor playing critical roles in the regulatory function in Treg. Cells stimulated with 1 nM of MK-0 enhanced FoxP3 protein amount, with elevated MFI of 451 from the PBS control value of 159. However, the same dose of MK-6 induced a

negligible increase in FoxP3 MFI (170), suggesting that MK-6 is a poor FoxP3 inducer for committed Tregs (Figure 3C). Taken together, we found MK-6 possesses attenuated stimulating effects on Treg.

## 3.4 MK-6 administration induced elevation of CD8+ T to Treg ratio in spleen compared with IL-2

Next, we asked whether MK-6 has a weaker Treg expansion potential than MK-0 in vivo. We intraperitoneally administered the Mutakines to tumor-free mice and analyzed splenic immune cells (Figure 4A). Low-dose MK-0 (25 μg/head, once daily for four consecutive days) induced a mild increase of FoxP3$^+$CD25$^+$ Treg, and we saw a significant growth of Treg after the 250-μg treatment (Figure 4B). However, dose escalation studies with MK-6 showed slight Treg expansion, remaining almost unchanged from the PBS controls. We also examined splenic CD8$^+$ T and DX5$^+$ CD3$^-$ NK cells. Somewhat unexpectedly, we did not find any difference between MK-0 and MK-6 in the two cell populations' expansion (Figure 4C,D). Finally, we evaluated the CD8$^+$ T to Treg ratio, indicative of a cytotoxic immune environment. The low-dose MK-0 (25 μg) treatment exhibited a mild decrease in the CD8$^+$ T to Treg ratio, and we observed a significant reduction by the high-dose MK-0 (250 μg) administration. However, the CD8$^+$ T to Treg cells ratio did not decline even by the same high amount of MK-6 (Figure 4E). Collectively, these results demonstrate that MK-6 possesses the capability to upregulate the CD8$^+$ T to Treg ratio in vivo.

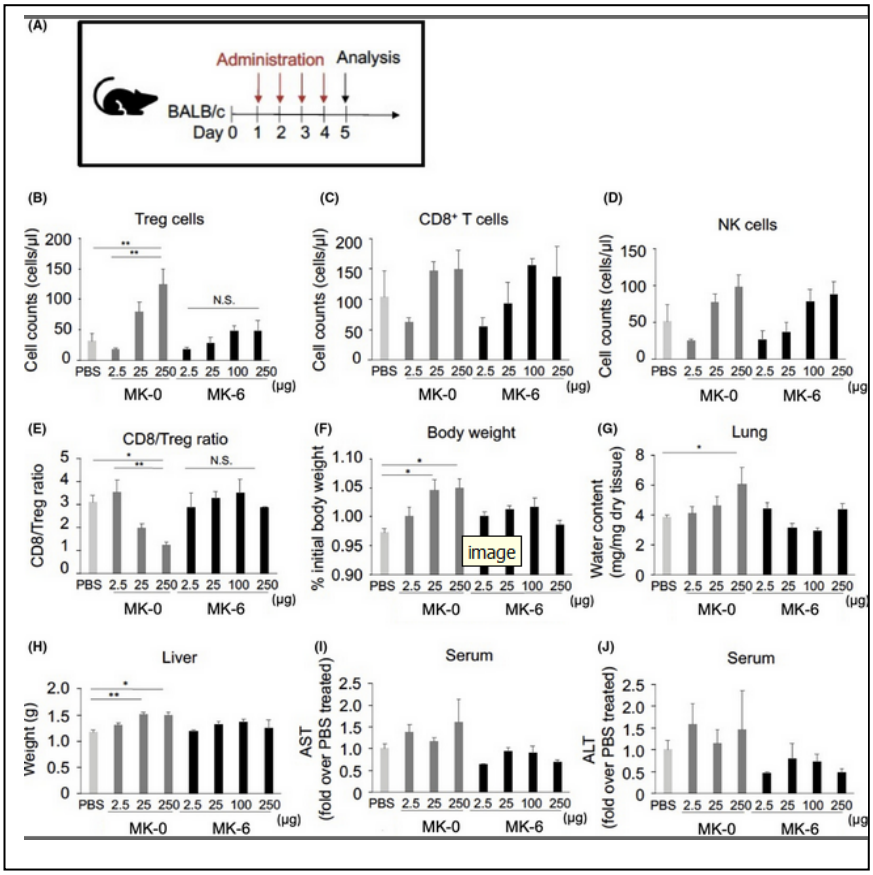


**FIGURE 4**
Open in figure viewerPowerPoint
MK-6 exerts fewer adverse effects and a higher CD8$^+$ T to Tregs ratio. A, BALB/c mice received intraperitoneal administration of MK-0 or MK-6 (5 μg) once a day on days 1-4, and splenocytes were analyzed by FACS on day 5 (B-E). B, Cell counts of Treg (FoxP3$^+$CD25$^+$ of CD4$^+$CD3$^+$), CD8$^+$CD3$^+$ T (C), NK (DX5$^+$CD3$^-$) (D), and the CD8$^+$ T to Tregs ratio (E). F-J, Adverse effect analysis on day 5. F, Bodyweight is represented as the percentage of initial body weight. G, Pulmonary edema was assessed by measurement of lung water content. H, We harvested and weighed the liver and measured the serum AST (I) and ALT activities (J). n = 5 (MK-0 group), n = 3 (others), n = 7 (PBS group in G, I, and J). Data show means + SEM. NS, not significant

## 3.5 MK-6 decreased IL-2 administration–associated adverse effects in mice

IL-2Rα has a broad expression profile, most notably on vascular endothelial cells. Because MK-6 had lost IL-2Rα–binding ability, we expected that MK-6 would reduce toxicity associated with IL-2 administration. To evaluate the correlation between MK-6's IL-2Rα–binding capacity and adverse effects in vivo, we administered titrated doses of MK-0 and MK-6 to tumor-free mice (Figure 4A,F-J). We evaluated mice for body weight, pulmonary edema, and hepatic function. All of them consist of hallmarks

of IL-2 therapy–associated adverse effects called experimentally induced VLS.[13, 24, 25] MK-0 treatment induced body weight gain, pulmonary edema, and liver weight increase in a dose-dependent manner (Figure 4F-H). By contrast, we barely observed these adverse effects in mice injected with MK-6, remaining largely asymptomatic like the PBS controls. Two markers for liver injury, AST and ALT, revealed no differences to controls across all treatment groups (Figure 4I,J). Together, these results indicate that MK-6 administration does not induce severe systemic toxicity, often associated with IL-2 immunotherapy.

### 3.6 MK-6 immunotherapy is efficacious in syngeneic tumor models

Next, we examined the antitumor efficacy of MK-6 using mouse syngeneic tumor models. First, CT26 tumor–bearing mice were administered 25 μg of MK-0 and MK-6 once daily for seven consecutive days (Figure S13). However, this equal dose of MK-6 and MK-0 did not significantly affect CT26 tumors, irrespective of the IL-2Rα binding. Besides, before the assay, all the mice injected with 25 μg of MK-0 manifested lower robustness, such as shivering and less mobility (data not shown). A dose escalation study achieved an excellent $CD8^+$ T cells to Treg ratio by 100 μg MK-6 (Figure 4E). The T cell proliferation potential of MK-6 was much lower than that of MK-0 (Figure 1C,D); we adjusted the dosage of MK-0 so that it exerts the same $EC_{50}$ value against trimeric αβγ IL-2Rs with that of MK-6. Altogether, 5 μg of MK-0 or 100 μg of MK-6, equivalent amounts for the high-affinity IL-2Rs, were injected twice a day intraperitoneally into the CT26 tumor–bearing mice (Figure 5A). MK-6 injection induced slight retardation of tumor growth on day 7 and significant tumor volume suppression on day 11, compared with PBS controls and MK-0. All the mice were devoid of unhealthy conditions throughout the experiments, suggesting that the respective doses of MK-6 and MK-0 were tolerable. We also monitored adverse effects on day 12. MK-0–treated tumor-bearing mice significantly increased liver weight compared with those with PBS or MK-6 injection (Figure S14A), but serum AST and ALT levels remained unaltered (Figure S14B,C). By contrast, both MK-6 and MK-0 induced body weight gain (Figure S14D), and neither MK-6 nor MK-0 treatment induced pulmonary edema (Figure S14E). Collectively, MK-6 treatment at the $EC_{50}$-referenced dose exhibited therapeutic effects in the CT26 syngeneic tumor model, and we managed to avoid the adverse impact of high-dose MK-6.

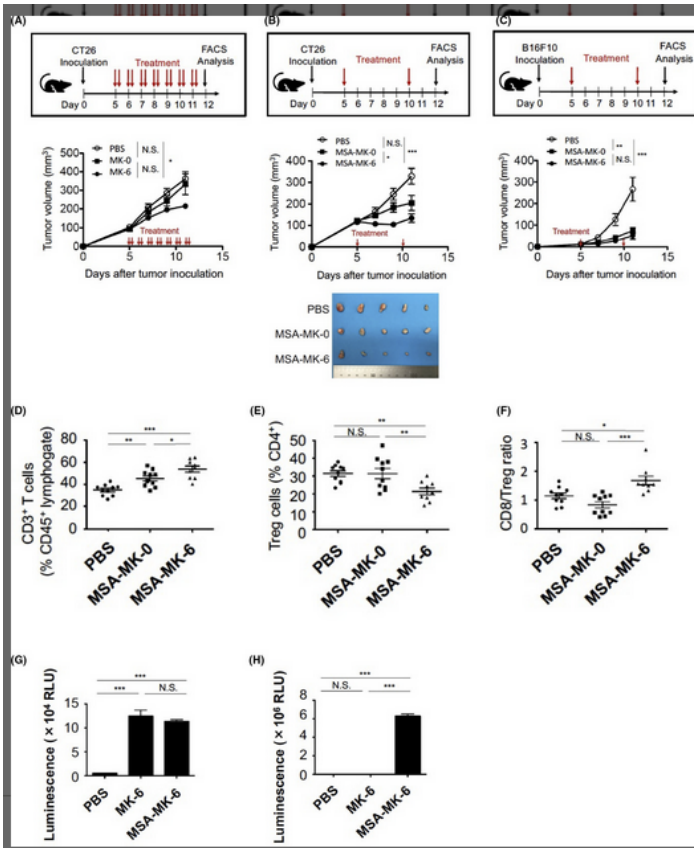


**FIGURE 5**

Open in figure viewerPowerPoint

MK-6 and maximum serum concentration of albumin-fused MK-6 (MSA-MK-6) exert an antitumor effect in the CT26 and B16F10 tumor models. Tumor-bearing BALB/c or C57BL/6 mice received intraperitoneal administration of (A) MK-0 (5 μg), MK-6 (100 μg), or PBS twice a day, starting on day 5 after tumor implantation, or (B and C) MSA-MK-0 (10 μg), MSA-MK-6 (200 μg), or PBS on day 5 and 10. n = 10-13 per group from two independent experiments. Mean tumor size ± SEM. NS, not significant. Dissected CT26 tumors in (B). D-F, CT26 tumors were harvested on day 12, followed by FACS analysis for (D) the frequency of $CD3^+$ T cells of $CD45^+$ lymphocyte, (E) Tregs ($FoxP3^+CD25^+$) of $CD4^+CD3^+$ T cells, and (F) the $CD8^+$ T cells to Tregs ratio. n = 10 (PBS), n = 10 (MSA-MK-0), n = 9 (MSA-MK-6). Data from two independent experiments are shown as means ± SEM. G, In vitro binding assay of MSA-MK-6 and MK-6 on CT26

cells. n = 4 per group. H, Intra–CT26 tumor uptake of MSA-MK-6. Tumor-bearing BALB/c mice received intraperitoneal administration of MSA-MK-6 (260 μg) and MK-6 (100 μg), and we harvested tumors 24 h later. We then assayed, minced, and lysed specimens for luciferase activities (means + SEM). n = 6 per group

### 3.7 Albumin-conjugated MK-6 improved pharmacodynamics while maintaining therapeutic functions

One of the disadvantages of IL-2 therapy is its short half-life in vivo, less than 30 minutes.[26, 27] We noticed that the addition of NanoLuc to IL-2 may moderately affect IL-2's longevity, which was still not satisfactory. We selected mouse serum albumin (MSA) to stabilize Mutakines and avoid potential outcomes from the artificial fusion partner. We fused it to the C-terminus of MK-6 via a flexible linker (Figure S1B). The serum half-life of MSA-MK-6 (5.6 hours) was approximately twice that of MK-6 (2.9 hours), and we could detect MSA-MK-6 up to 120 hours after the intravenous injection, resulting in its 15 times higher estimated AUC than that of MK-6 (Figure S15A,B). We next examined the in vivo effect of MSA-MK-6 using tumor-bearing mice. Considering the 20-fold difference in high-affinity IL-2 binding, we determined dosing conditions for MSA-MK-6 and MSA-MK-0 to exert equivalent effects of IL-2 signaling. Also, our preliminary experiments have suggested an extension of the intraperitoneal administration interval of MSA-MK-6 up to 96 hours. Accordingly, CT26 tumor–bearing mice received two intraperitoneal injections of 10 μg of MSA-MK-0 or 200 μg of MSA-MK-6 on days 5 and 10 after the tumor implantation (Figure 5B). All the mice tested remained healthy throughout the study. MSA-MK-0 and MSA-MK-6 significantly suppressed the growth of CT26 tumors, and the efficacy of MSA-MK-6 was comparable to that of MSA-MK-0. We also checked B16F10 melanoma tumors. The MSA-MK-6 and MSA-MK-0 showed similarly high efficacy compared with that of PBS (Figure 5C). The tumor-infiltrating lymphocyte (TIL) analysis revealed that MSA-MK-6–treated CT26 tumors contained substantially more $CD3^+$ T cell populations (Figure 5D). In contrast, $FoxP3^+CD25^+$ Treg infiltration was attenuated considerably by the MSA-MK-6 treatment, compared with the same population by the MSA-MK-0 or PBS (Figure 5E). MSA-MK-6 treatment enhanced the $CD8^+$ T cells to Treg cells ratio in TILs, compared with PBS or MSA-MK-0 treatments (Figure 5F). Using a fusion partner albumin, MK-6 increased its stability and exerted its antitumor activity in vivo even by the 4-day-interval administrations. Furthermore, albumin may contribute to tumor targeting of MK-6. To examine such drug delivery effects, we used NanoLuc-fused MSA-MK-6 to observe pharmacokinetics. First, we asked for direct binding of MSA-MK-6 to tumor cells, but it did not show an increase in any association with CT26 in vitro (Figure 5G). We next proceeded to the in vivo study. MK-6 or MSA-MK-6 was injected intraperitoneally into the CT26 tumor model. Twenty-four hours after injection, we harvested the tumors and measured the luciferase activities. The intratumor uptake of MSA-MK-6 was considerably higher than that of MK-6 (Figure 5H). These data demonstrate that a significant amount of MSA-MK-6 remains within the tumor even 24 hours after injection.

## 4 DISCUSSION

Here, we developed a genetically modified IL-2, MK-6, with partial T cell proliferation potential. By diminishing the IL-2Rα binding, MK-6 gained two significant advantages. First, MK-6 administration reduced inevitable toxicity associated with high-dose IL-2 therapy. Second, MK-6 attenuated anti-immunogenic Treg expansion. Accordingly, MK-6, especially when fused with albumin, exerted an antitumor effect in syngeneic mouse tumor models without apparent significant adverse effects.

We designed MK-6 carrying four mutations over the aldesleukin-type IL-2. There are several attempts to manipulate IL-2 in terms of altering their specific target cell populations. NARA1 is a monoclonal antibody that occupies the CD25 epitope of IL-2 by binding to the loop-AB, helix-B, and loop-BC, and the IL-2-NARA1 complex preferentially stimulates $CD8^+$ T cells rather than Tregs.[28] Likewise, anti-mouse IL-2 antibody S4B6/mouse IL-2 complex selectively promoted proliferation of effector T cells.[29] Alternatively, PEG conjugation has been applied to IL-2, leading to $CD8^+$ T cell increase. NKTR-214 is

an aldesleukin conjugated with six PEG chains at K31/K34/K42/K47/K48/K75 residues, allowing its preferential interaction IL-2Rβ, but not IL-2Rα. As there is a concern about the production of anti-PEG antibodies for immunogenicity,[30] modifying IL-2 itself by amino acid substitutions is attractive in this sense. A superkine H9 super-2 and IL-2 mutant with a set of L80F/R81D/L85V/I86V/I92F in loop-BC and helix-C shows increased IL-2Rβ affinity and decreased IL-2Rα binding. This IL-2 mutein preferentially expands cytotoxic lymphocytes rather than Treg.[22] In our hands, MK-19 carrying the same mutations (L80F/R81D/L85V/I86V/I92F) showed partial IL-2Rα binding but enhanced cell growth potential toward IL-2Rβγ–positive cells, suggesting this mutein itself possesses a Treg proliferation potential. Interestingly, an IL-2 mutant with a single F42A mutant in loop-AB showed decreased IL-2Rα binding without affecting the IL-2Rβ binding[31, 32] and in the present study, introducing alanine, carrying the most petite side chain among amino acids, to the aldesleukin's four positions at K35/R38/K43/Y45 successfully disabled MK-6 to interact with the IL-2Rα. The alanine-substituted mutant approach is distinct from the one used for NKTR-214. No bulky mass interferes with the IL-2/IL-2Rα interaction instead of creating a space wide enough for abrogating hydrogen bonds and Van der Waals forces. Two previously reported IL-2 muteins, MK-9 and MK-18, also abolished the same loop-AB of IL-2 to disable IL-2Rα binding in the 3D analyses by combining mutations (data not shown). Surprisingly, however, MK-9 and MK-18 have lost murine T cell growth potential (Figure S11G) while maintaining human T cell growth. We speculate mutations on the IL-2: IL-2Rα interface may have affected the whole structure of IL-2. In our 3D structure analysis, together with the fact that IL-2Rβγ–positive T cells grew with similar efficiency, we speculate that MK-6 maintains the original four-barrel structure of IL-2.

MK-6 has an advantage in reducing toxicity over aldesleukin, a conventional IL-2 in clinical use. IL-2 administration is an attractive treatment option for metastatic renal cell carcinoma and melanoma. However, severe toxicity has narrowed its common usage. High-dose IL-2 immunotherapy often leads to VLS, with increased vascular permeability in systemic organs such as lungs and liver, resulting in fatal pulmonary edema and hepatic dysfunction.[33, 34] Because the pulmonary edema is relieved by a blocking antibody to IL-2Rα, direct interaction of IL-2 with IL-2Rα on endothelial cells is the underlying pathophysiology for VLS,[13] and neutralizing or disabling this interaction has been a concern for therapeutic development.[21, 35] An IL-2/anti-IL-2Rα hybrid reduced pulmonary edema, and a superkine H9 super-2 caused substantially less pulmonary edema than the mixture. In comparison, pulmonary edema induced by MK-6 seems to be minimal among the three. On the other hand, high dose IL-2/NARA1 complexes induced pulmonary edema.[28] The weaker pulmonary edema by MK-6 may be due to the multiple interaction abrogation between MK-6 and IL-2Rα, which may enable a possible application of an even higher-dose MK-6–based immunotherapy.

We speculate MK-6 worked efficaciously in vivo because it increases the $CD8^+$ T to Treg ratio within tumors. The immune system in the tumor microenvironment (TME) is often associated with therapeutic resistance.[36] In clinical practice, accumulating evidence suggests that infiltration of a large number of Tregs into tumor tissues and the lymph node is associated with inadequate clinical responses[37, 38] Skewing the immune cell balance to favor $CD8^+$ T over Treg would improve therapeutic efficacy.[14, 39-41] A crucial feature of Tregs is that they express high-affinity IL-2Rαβγ, yet they do not produce IL-2. Tregs, instead, highly rely on exogenous IL-2 produced by neighboring activated T cells for their survival and proliferation[42] via the JAK3/STAT5 signaling pathway.[43] IL-2Rα expression is enhanced in activated Tregs, creating a positive feedback mechanism to favor IL-2R$\alpha^+$ Tregs. On the contrary, IL-2–deprived $CD8^+$ T cells cannot proliferate due to the IL-2 consumption by Tregs. Accordingly, several reports have demonstrated a tight association of Treg proliferation with insufficient IL-2 therapy,[21, 35, 44] and Treg depletion improves IL-2–induced antitumor immunity. These results highly suggest that IL-2 immunotherapy demands a concomitant Treg suppression strategy.[45] Adding MK-6 to the TME should change the balance of $CD8^+$ T and Treg cells controlling the two cell populations' survival and functions. Interestingly, MSA-MK-6 administration increased $CD3^+$ and $CD8^+$ T cell infiltration in the TME. The albumin-fused MK-6 seems to alter immunologically “cold” tumors into “hot” and creates an antitumor environment by relatively reducing the effect of Treg in a desert-type TME.[46]

The stability of IL-2 has been another significant factor to improve the clinical efficacy, for IL-2 receives rapid renal clearance resulting in its short half-life.[26] In this study, we managed to give MK-6 durable stability by fusing it with serum albumin. Albumin has an extraordinary half-life of almost 3 weeks in vivo.[47] The maximum serum concentration of albumin-fused MK-6 (MSA-MK-6) was higher than that of MK-6, making a dramatic increase in the AUC. Accordingly, we could reduce the administration interval so that only two intraperitoneal shots of MSA-MK-6 worked even better for CT26 tumor shrinkage than series of twice-daily injections of its prodrug, MK-6.

Furthermore, albumin often accumulates at tumor sites and inflamed tissues.[47] These attractive properties of albumin make it favorable for its drug delivery vehicle.[48, 49] In sarcoma therapy, for instance, doxorubicin's cardiac toxicity has limited its clinical use. By conjugating with human serum albumin, aldoxorubicin (INNO-206) reduced cardiac toxicity and improved its tumor-specific accessibility.[50] In this study, MSA-MK-6 did not directly bind CT26 cells in vitro, but a substantial amount of MSA-MK-6 accumulated in CT26 tumors. Efficient albumin earnings within tumors have been well documented and termed the “enhanced permeability and retention of macromolecules (EPR) effect.”[51] The leakiness of cancer-associated endothelium explains the phenomenon of tumor interstitium and molecules' movement within fluids. Although our present works did not uncover an aspect of active MSA-MK-6 uptake into tumors, one could speculate that the EPR effect might elevate its intratumor transport. The pronounced antitumor activity of MSA-MK-6 suggests that it is an attractive agent to induce antitumor immunity with relatively long bioavailability.

The present study's main limitations are the different weight doses of modified IL-2, affecting the therapeutic outcomes. Our experimental design used 20 times more MK-6 than the prototype form MK-0 in the syngeneic tumor models. We designed the dosages so that each dosage supports equivalent growth and signaling on high-affinity IL-2R–expressing cells; differences adjusted for MK-6 and MK-0 considering (a) $EC_{50}$ in growth assays on trimeric αβγ IL-2Rs–expressing T cells and (b) pSTAT5 of Treg-like MT-2 cells. Notably, MK-6 did not cause any dose-dependent systemic toxicity associated with IL-2Rα, and the higher dose given to mice was well tolerable. Safety of high-dose MK-6 treatment would benefit from developing a new IL-2–associated therapy in the future.

In conclusion, we have developed a not-α IL-2, MK-6, devoid of IL-2's severe adverse effects in vivo. Albumin-fused MK-6 showed a significant antitumor impact by enhancing the CD8 to Treg ratio of the. Our current results of IL-2–based therapy may pave the way for the development of effective cancer immunotherapies.

## ACKNOWLEDGMENTS

This work was supported by Grants-in-Aid for Scientific Research (B) (18H02701) and (C) (18K08643, 18H04056, 19K08609, 20K08580, and 20K08203) from the Japan Society for the Promotion of Science, Grants-in-Aid from JST-CREST (JPMJCR17H4), and the Project for Cancer Research and Therapeutic Evolution from the Japan Agency for Medical Research and Development (21cm0106387h0001). We thank the Biomedical Research Core of the Tohoku University Graduate School of Medicine for technical support and H. Kosai and N. Ishizawa for technical assistance.

## DISCLOSURE

The authors declare that they have no competing interests.

## AUTHOR CONTRIBUTIONS

MK, KK, KM, TT, TF, and NT designed the research; MK, KK, KM, YA, and NT wrote the paper; MK, KT, and KK performed cell culture, molecular biology, and several experiments; and KM provided 3D data analyses.